Piezotronic-Effect Enhanced Drug Metabolism and Sensing on a Single ZnO Nanowire Surface with the Presence of Human Cytochrome P450

Ning Wang,[†,§,#] Caizhen Gao,[†,§,#] Fei Xue,[‡] Yu Han,[‡,§] Tao Li,[‡] Xia Cao,[*,†,‡] Xueji Zhang,[*,†] Yue Zhang,[†] and Zhong Lin Wang[*,‡,∥]

[†]School of Chemistry and Biological Engineering, University of Science and Technology Beijing, Beijing, 100083, China, [‡]Beijing Institute of Nanoenergy and Nanosystems, Chinese Academy of Sciences, Beijing, 100083, China, [§]School of Chemistry and Environment, Beijing University of Aeronautics and Astronautics, Beijing, 100191, China, and [∥]School of Material Science and Engineering, Georgia Institute of Technology, Atlanta, Georgia 30332-0245, United States. [#]These authors (N.W. and C.G.) contributed equally to this work.

ABSTRACT Cytochromes P450 (CYPs) enzymes are involved in catalyzing the metabolism of various endogenous and exogenous compounds. A rapid analysis of drug metabolism reactions by CYPs is required because they can metabolize 95% of current drugs in drug development and effective therapies. Here, we describe a study of piezotronic-effect enhanced drug metabolism and sensing by utilizing a single ZnO nanowire (ZnO NW) device. Owing to the unique hydrophobic feature of a ZnO NW that provides a desirable "microenvironment" for the immobilization of biomolecules, our device can effectively stimulate the tolbutamide metabolism by decorating a ZnO NW with cytochrome P4502C9/CYPs reductase (CYP2C9/CPR) microsomes. By applying an external compressive strain to the ZnO nanowire, the piezotronic effect, which plays a primary role in tuning the transport behavior of a ZnO NW utilizing the created piezoelectric polarization charges at the local interface, can effectively enhance the performance of the device. A theoretical model is proposed using an energy band diagram to explain the experimental data. This study provides a potential approach to study drug metabolism and trace drug detection based on the piezotronic effect.

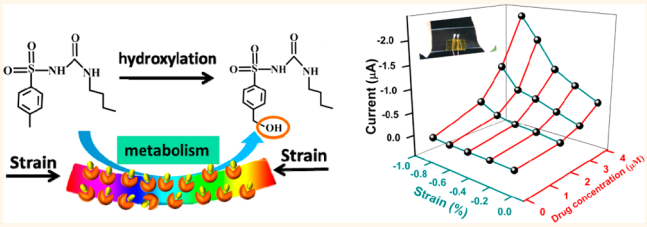

KEYWORDS: piezotronic effect · drug metabolism · ZnO nanowire · cytochrome P450

Cytochromes P450 (CYPs) are a large family of auto-oxidizable heme proteins that are found in almost all types of organisms and play an essential role in the metabolism of most drugs and chemicals.[1−3] As a member of the CYP family, cytochrome P450 2C9 (CYP2C9) is involved in the oxidation of approximately 16% of therapeutically important drugs.[4] However, in the process of drug metabolism mediated mainly by CYPs, interactions between drug−drug/drug−food can result in toxicities and other effects.[5,6] Therefore, it is necessary to study drug metabolism reactions using CYPs to identify the associated issues such as in the field of drug development.

In vivo, CYPs catalyze drugs *via* a typical cycle of electron delivery from nicotinamide adenine dinucleotide phosphate (NADPH) to CYPs reductase (CPR) for subsequent delivery to CYPs heme (the active center of CYPs consists of an iron protoheme that is activated *via* electron transfer reactions).[7] On the basis of this mechanism, numerous studies have been carried out to explore the drug metabolic pathway by use of different systems, such as biocatalytic systems, electrochemically driven enzymatic system, electrochemical oxidation systems, and other types of *in vitro* systems.[8] In the last decades, electrochemical systems had attracted extensive interest because the electrode could be used as an alternative electron source, instead of a high-cost conventional electron-supply source (NADPH), for providing an easy and economic method for CYPs catalysis metabolite formation

* Address correspondence to caoxia@ustb.edu.cn, zhangxueji@ustb.edu.cn, zlwang@gatech.edu.

Received for review January 8, 2015 and accepted March 10, 2015.

Published online 10.1021/acsnano.5b00142

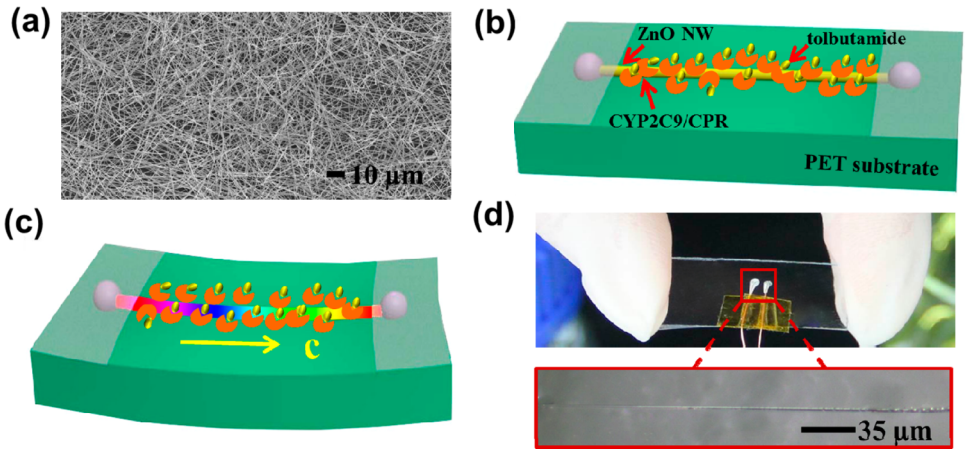

Figure 1. (a) Scanning electron microscopy (SEM) image of the as-synthesized ZnO NWs. Schematic of ZnO NW decorated with CYP2C9/CPR-microsomes combined with tolbutamide molecules under (b) no strain and (c) compressive strain. (d) Optical images of a fabricated ZnO NW device.

in vitro. In 2005, electron transfer occurring *via* CPR molecules to recombinant CYP1A2 and CYP3A4 enzymes was proposed by Rusling *et al*. but lacked experimental proof.[9] The same group reported electrochemical probing of interactions between CPR and CYP molecules in 2011.[10] Gilardi and his co-workers immobilized CYP2C20 on a gold electrode modified with gold nanoparticles to study the activity of CYP2C20.[11] Liu's group constructed a mixed film containing indium−tin-oxide nanoparticles (ITO NPs) and CYP2C9/CPR-microsomes on a glassy carbon electrode to drive the drug metabolism *via* electrochemical method.[7] Nevertheless, application of these systems has to face some difficulties, such as adsorptive denaturation of proteins, rate limited diffusion of substrate to the electrode, structural changes of enzyme during immobilization, and a lipid bilayer environment.[12,13] Most of all, an external power source is mandatory for stimulating the process.

Remarkable achievements in the field of drug metabolism can be attributed to applications of nanomaterials, which control CYP orientation or form an electron transfer path.[14] The list of nanocomposites consists of ITO NPs,[14] colloidal gold/graphene nanocomposites,[15] and carbon nanofibers,[16] and so on. Among nanomaterials, ZnO, one of the wurtzite structured semiconductors, exhibits the piezotronic effect that uses strain-induced piezopotential as a "gate voltage" for tuning/controlling the local Schottky barrier height (SBH) across an interface/junction within a piezoelectric device.[17] Therefore, the performance of ZnO-based nanodevices can be enhanced by the piezotronic effect for UV sensors, strain sensors, and photodetectors.[18−20] In addition, nanostructured ZnO materials possess high surface area, no toxicity, and good biocompatibility,[21,22] and therefore have great potential applications in biosensors and biomedicine.[23−25] What's more, ZnO nanomaterials exhibit unique hydrophobic features that could provide a desirable "microenvironment" for the immobilization of biomolecules such as enzymes, DNA, antibodies, *etc*. and preserve the bioactivity of the immobilized materials, which qualify it as a good matrix for biomolecules immobilization.[26,27] Up to now, lots of research about ZnO nanomaterials biosensors have been reported.[28−30]

In this paper, we present the first study of piezotronic effect enhanced drug metabolism at the surface of a single ZnO NW, which is decorated with CYP2C9/CPR-microsomes. Our results indicate that the piezopotential produced by ZnO NW, under a static applied external strain, could effectively promote drug metabolism. A theoretical model is proposed using the energy band diagram to explain the observed behaviors.

RESULTS AND DISCUSSION

ZnO Nanowires Synthesis and Characterization. ZnO nanowires were synthesized using a solid−vapor process at high temperature[31−33] (Figure 1a). A schematic in Figure 1b displays a strain free ZnO NW device decorated with CYP2C9/CPR-microsomes combining with tolbutamide molecules, which is one of the typical CYP2C9 drug substrates, and CYP2C9 is essentially involved in the hydroxylation process of tolbutamide. Moreover, tolbutamide is widely accepted as a prototype substrate for the assessment of CYP2C9 activity, both *in vivo* and *in vitro*.[34] The same device on which external strain was applied is shown in Figure 1c. As shown in Figure 1d, optical images of the practical fabricated ZnO NW device were obtained by utilizing stereoscopic microscope (SZ660TP).

To characterize the hydrophobicity of the nanowires, 2 μL of distilled water was dripped onto the NW surface using a suitable microsyringe. It can be seen that the droplets stand on its surface (Figure 2a). Because of its excellent film forming ability, chitosan (CS) was used to functionalize microsomes for obtaining well-dispersed homogeneous microsomes−CS solution. After this solution was dropped onto the surface

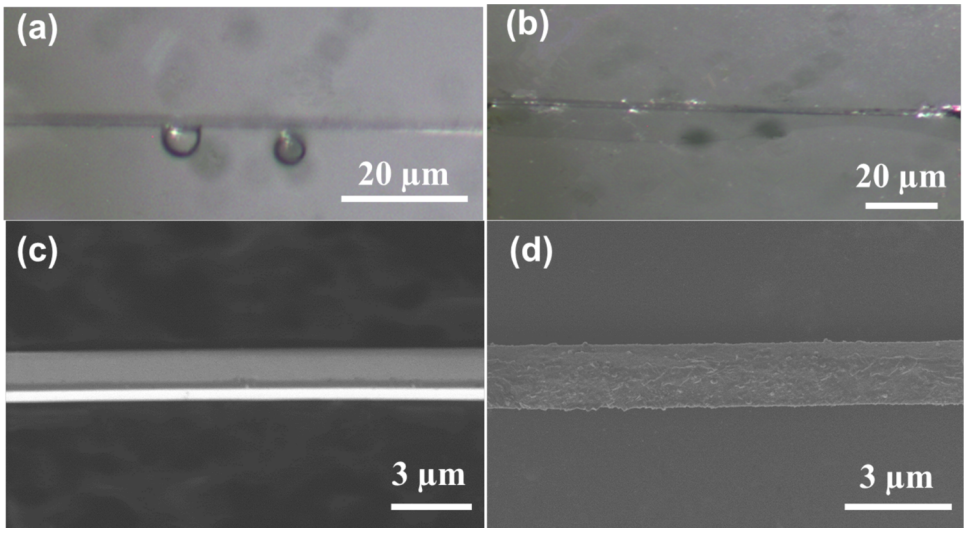

Figure 2. Optical microscopy images of ZnO NW on which a water-drop was dripped (a) and ZnO NW decorated with CYP2C9/CPR-microsomes (b). (c, d) SEM images of single ZnO NW before and after being decorated with CYP2C9/CPR-microsomes.

of the ZnO NW, a layer of uniform microsomes−CS film was formed (Figure 2b). Although it is known that ZnO may be self-dissolved by solution after some time, we found that this process was rather slow and it did not affect our measurement results. To better show the successful immobilization of microsomes on the surface of ZnO nanowire, the size and morphology of the nanowires were examined by SEM. Figure 2c shows that the ZnO NW had a smooth surface before being decorated with CYP2C9/CPR-microsomes. However, decoration with CYP2C9/CPR-microsomes can result in a ZnO NW with a rough surface, as presented in Figure 2d. All of these results demonstrated satisfactory immobilization microsomes on individual ZnO nanowires.

Performance Characterization of ZnO NW Device. The piezotronic effect enhanced drug metabolism was investigated by gradually applying a compressive strain on the ZnO NW device along the nanowire direction when it is totally immersed into the different concentration of tolbutamide solutions. As shown in Figure 3a, *I*−*V* curves of the ZnO NW device decorated with different substances under −0.39% strain were obtained. The output signals were weak when the fabricated device was without any decoration or when the undecorated device was immersed into tolbutamide solution. However, a high current response was observed when the ZnO nanowire device was decorated with CYP2C9/CPR-microsomes. Furthermore, a higher current was obtained when the decorated ZnO NW device was immersed into the tolbutamide solution. A significant difference was observed between the current signal obtained in the absence and presence of CYP2C9/CPR-microsomes. This also confirmed that CYP2C9/CPR-microsomes are essential to facilitate target drug metabolism based on the piezotronic effect. The experimental facility consists of a three-dimensional mechanical stage with movement resolution of 1 μm (Figure 3b). One end of the device was firmly affixed on a manipulation holder that was to be bent, while the other end was set free to apply a strain. The compressive strain can be derived according to the previously reported methode.[35] To better understand the piezotronic effect on drug metabolism, four drawings were given to show the response of ZnO NW device under different compressive strain with a bias voltage from −1.1 to 1.1 V in Figure 3c−f. The response of a ZnO NW device in pH 7.4 PBS solution under different compressive strains without combining with tolbutamide molecules was measured (Figure 3c). The overall output signals were increased slightly. However, the response signals of the device increased significantly with the increase of tolbutamide concentrations from 0 to 4 μM (Figure 3c−f). This result demonstrated that the CYP2C9 isozyme-decorated ZnO NW device had a sound response to tolbutamide. For example, Figure 3e depicts the *I*−*V* characteristics of a device when the externally applied different compressive strains increased from 0%, −0.19%, −0.43%, −0.62% to −0.80% with 3 μM tolbutamide. We can see that at a bias voltage of 1.1 V, the output signals increased from 0.638 μA to more than 5.4 μA, which is an ∼9 times increase after applying −0.80% compressive strain. Similar trends were observed for all of the *I*−*V* curves.

To systematically analyze the ZnO NW device response to constantly changing compressive strains and target drug concentration at a fixed bias voltage of −0.4 V, a three-dimensional (3D) graph was plotted, as depicted in Figure 4a. An overall changing trend of current signals with a difference of compressive strains and tolbutamide concentrations can be simultaneously calculated from this 3D graph. We can see that current obviously increased as the compressive

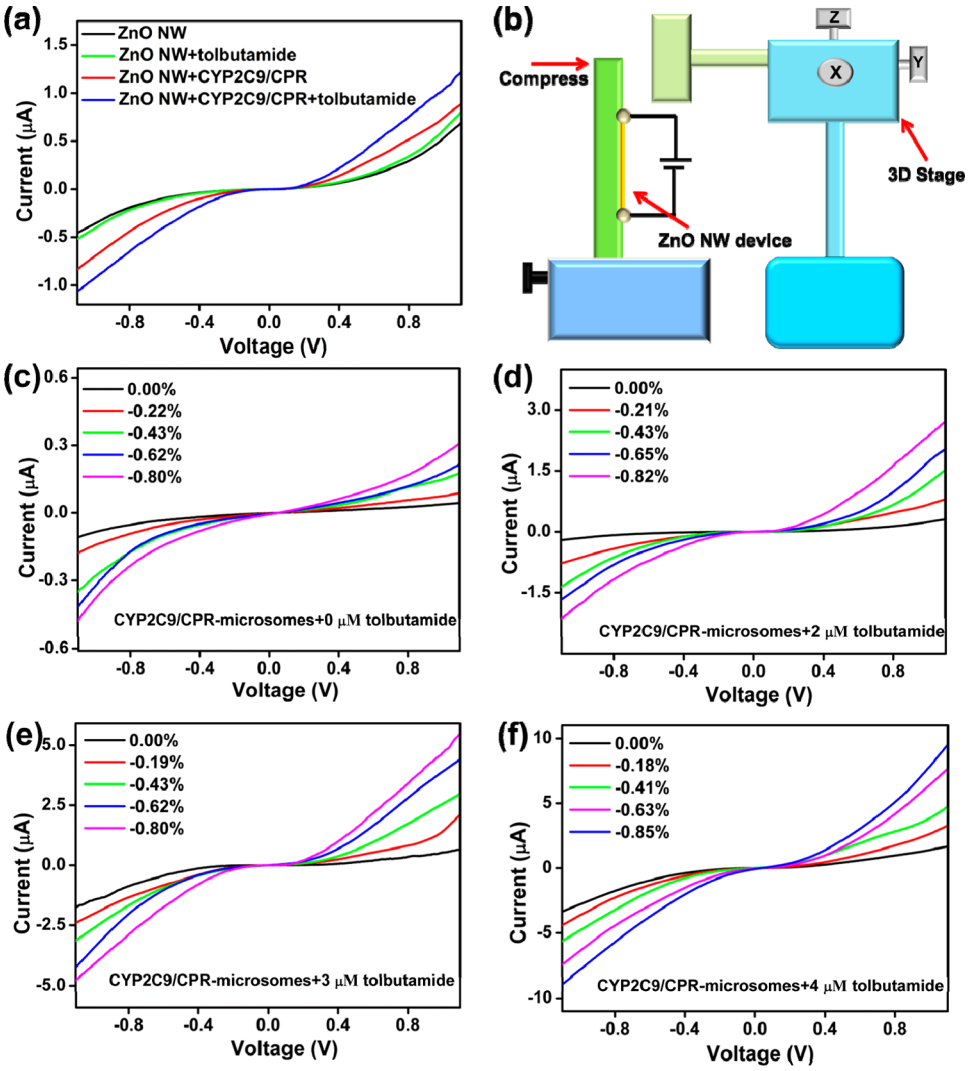

Figure 3. (a) *I*−*V* curves of the ZnO NW device in pH 7.4 PBS solution under approximately −0.39% strain with a bias voltage from −1.1 to 1.1 V, decorated with nothing (black solid line), nothing, but in the presence of tolbutamide molecules (green solid line), CYP2C9/CPR-microsomes (red solid line), CYP2C9/CPR-microsomes combining with tolbutamide solution (blue solid line). (b) Schematic diagram of the experiments setup, a three-dimensional mechanical stage. *I*−*V* characteristics of the ZnO NW device in pH 7.4 PBS solution under different compressive strains with a bias voltage from −1.1 to 1.1 V, when the device was decorated with (c) CYP2C9/CPR-microsomes. (d) CYP2C9/CPR-microsomes combining with 2 μM tolbutamide solution, (e) CYP2C9/CPR-microsomes combining with 3 μM tolbutamide solution, (f) CYP2C9/CPR-microsomes combining with 4 μM tolbutamide solution.

strains or tolbutamide concentrations increased. Four 2-dimensional (2D) graphs are presented in Figure 4b−e for more details, which are generated from Figure 4a by projecting on the I-strain surface and the I-drug concentration surface, respectively.

Figure 4 panels b and c illustrate the absolute and relative current response of CYP2C9/CPR-microsomes decorated ZnO NW device to different external strains, ranging from 0% to −0.8%, while concentration of tolbutamide was fixed at 0, 2, 3, 4 μM in every curve. All curves were obtained by measuring the transport current of the device under different compressive strains. The results indicate that increasing the compressive strain results in an enlarged output signal, which again proved that the performance of the device can be enhanced by the piezotronic effect at different drug concentrations. What's more, with the increase of strain, the difference between currents at two adjacent drug concentrations is increased. For example, without applying external strain, the difference between currents at 2 μM drug and 3 μM drug was about 0.155 μA, while the differences under −0.62% strain went up to 0.42 μA, which was more than 150% increase in magnitude. In Figure 4c, the relative change in current was up to 420%, when applied increasing compressive strain. The results indicated that the sensitivity of the ZnO NW device can be significantly enhanced by the piezotronic effect and may serve as a sensor for drug detection. Certainly, the high sensitivity is also attributed to the nonlinear *I*−*V* transport characteristics as for the Schottky barrier at the contacts of the M−S−M structure. Likewise, Figure 4 panels d and e reveal the

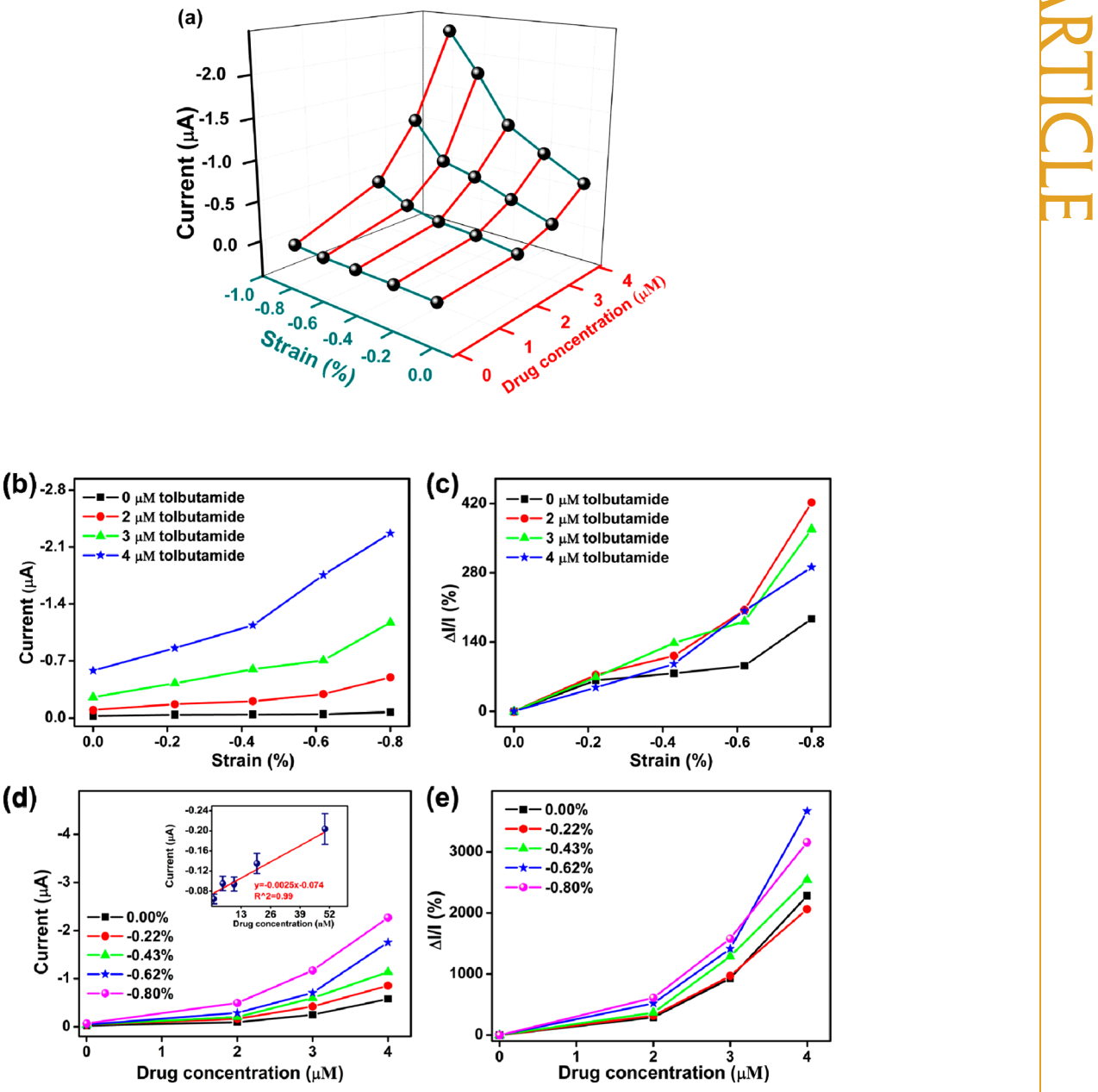

Figure 4. Piezotronic effect on the performance of ZnO NW device. (a) 3D graph illustrating the current response of the device in pH 7.4 PBS solution under different strains and tolbutamide concentrations at a fixed bias voltage of −0.4 V. (b, c) Absolute current response and relative current change of the device under different compressive strains, with the tolbutamide concentration ranging from 0 to 4 μM. (d, e) Absolute current response and relative current change of the ZnO NW device at different tolbutamide concentrations, with compressive strain between 0 and −0.80%, respectively. The inset in graph d shows current response of the ZnO NW device under lower concentration of tolbutamide solution. Data of panels b−e were extracted from panel a.

absolute and relative current response of the decorated ZnO NW device to different concentrations of tolbutamide under certain compressive strain. The 2D graphs present five curves under different compressive strains, each of which was derived by measuring the transport properties of ZnO NW device at different concentrations of tolbutamide. It is clear that at a certain concentration of tolbutamide, the larger the compressive strain is, the higher is the current signal: at a very low tolbutamide concentration, under free strain, the output signal was too small to be detected, whereas when a strain was applied, the output current greatly enlarged and was detected. As shown in the inset of Figure 4d, the device has a good response to tolbutamide with −0.8% strain applied. The calibration plot presented a good linear relationship between the currents and the concentrations of tolbutamide in the range from 1 nM to 50 nM. The linear regression equation was expressed as $I = -0.074 - 0.0025 \times C_{drug}$ (nM) with a correlation coefficient of 0.99. The detection limit was estimated to be 0.13 nM at a signal-to-noise ratio of 3, which may be suitable for trace drug

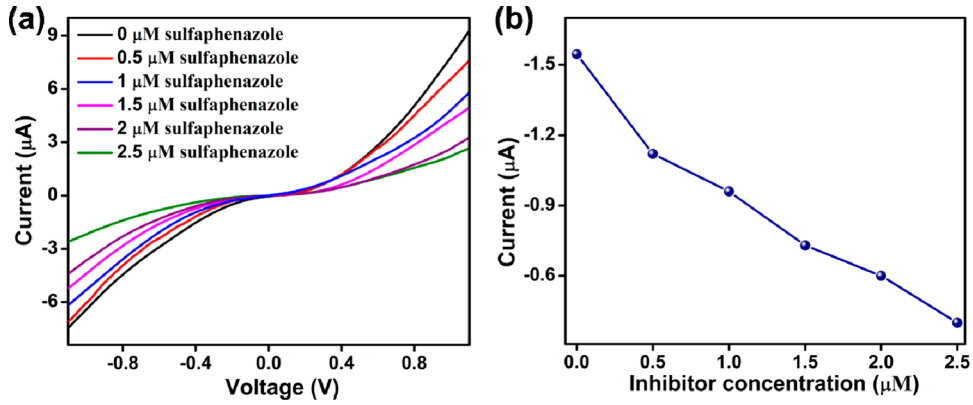

Figure 5. Analysis of inhibition effect on the metabolism of tolbutamide by sulfaphenazole. (a) *I*−*V* curves of the ZnO NW device decorated with CYP2C9/CPR-microsomes by the addition of different concentrations of sulfaphenazole in pH 7.4 PBS solution containing 4 μM tolbutamide under approximately −0.61% strain. (b) Current response of the device under different concentrations of sulfaphenazole.

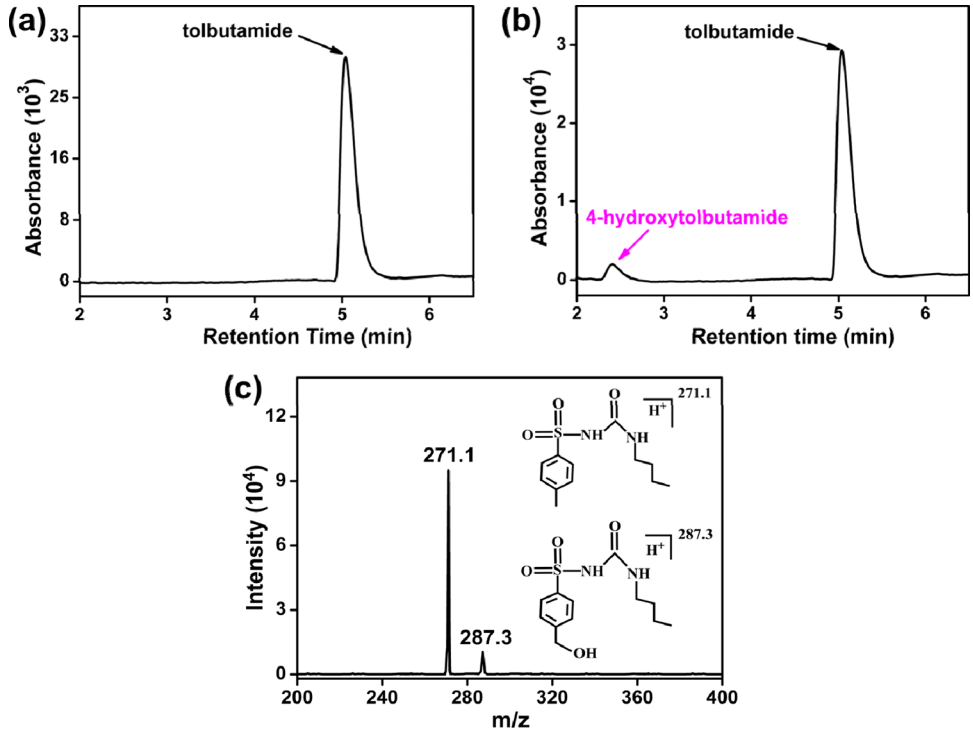

Figure 6. HPLC chromatograms of pure tolbutamide solution (a) and tolbutamide solution after metabolism driven by piezopotential (b). (c) Product ion spectra of the tolbutamide solution taken after the metabolism.

detection.[36,37] From the above, the proposed device is utilized to not only facilitate drug metabolism but also detect trace drug.

As a strong inhibitor of CYP2C9,[38] sulfaphenazole was used to study the inhibition effect on the hydroxylation of target drug in our experiment. As depicted in Figure 5a, *I*−*V* curves were acquired by varying inhibitor concentration (0, 0.5, 1, 1.5, 2, 2.5 μM) with 4 μM tolbutamide under −0.61% strain. As the concentration of sulfaphenazole in the solution increases, the current response of the ZnO NW device decreased. The current difference between the one without sulfaphenazole and the one with 2.5 μM sulfaphenazole reached to 1.05 μA (Figure 5b). This result can be attributed to the high-affinity of sulfaphenazole to CYP2C9.[39] That is to say, sulfaphenazole acts as a ligand to coordinate to CYP2C9 iron, which can lead to inhibiting the activity of CYP2C9 isozyme. Inhibition experiment further confirms that CYP2C9 immobilized on the surface of ZnO NW maintains its bioactivity.

To confirm drug metabolism reactions, high performance liquid chromatography (HPLC) and electrospray ionization-mass spectrometry (ESI-MS) analyses were conducted according to previous study.[7] The chromatogram of tolbutamide solution after metabolism with two peaks at 5.033 and 2.47 min was obtained, while just one peak was found at 5.04 min of pure tolbutamide solution (Figures 6a,b). So, the peak at 2.47 min

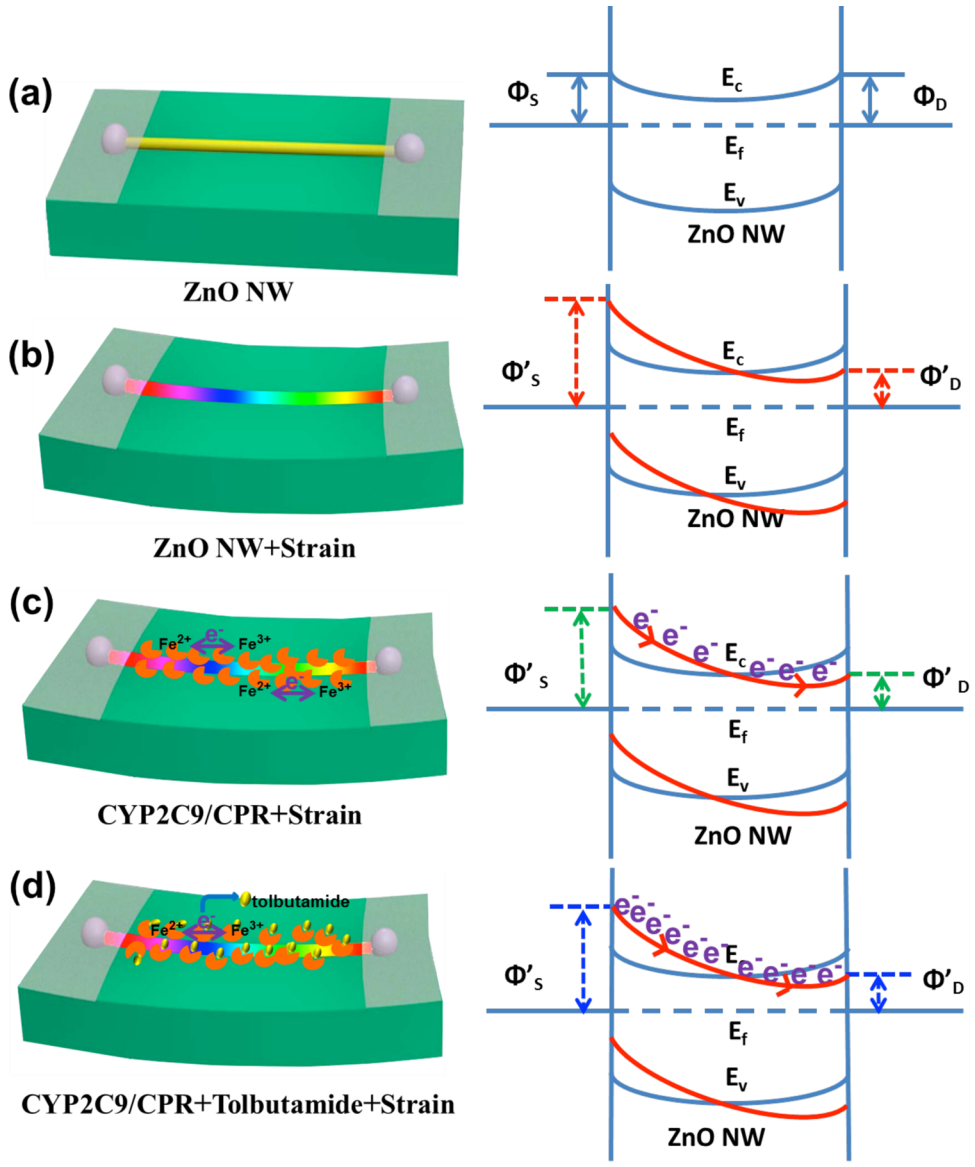

Figure 7. Schematic energy band diagrams of a ZnO nanowire device, illustrating the change of Schottky barrier height at the source and drain contacts when they are (a) unstrained, shown as blue solid lines in the graph on the right; (b) compressively strained, shown as red dashed lines; (c) compressively strained and decorated with CYP2C9/CPR-microsomes, but without tolbutamide solution, shown as green dashed lines, arrows indicate the direction of electrons movement; (d) compressively strained and decorated with CYP2C9/CPR-microsomes, combining with tolbutamide molecules, shown as blue dashed lines, arrows indicate the direction of electrons movement.

was assigned to the polar 4-hydroxytolbutamide, which is a strong polar substance, moving faster in a polar mobile phase. To analyze the products, ESI-MS was also utilized. As depicted in Figure 6c, the reaction products showed another peak at *m/z* 287.3, which corresponded to the molecular ion of 4-hydroxytolbutamide. Meanwhile, there was only one peak at *m/z* 271.1 for pure tolbutamide solution in its spectrum. The results indicated that the metabolism process generates 4-hydroxytolbutamide from tolbutamide.

Interpretation of Data. As for ZnO NW, the transport process of charge carriers can be tuned at the metal–semiconductor contact by two effects: piezoresistive effect and piezotronic effect, which coexist for the data presented in Figure 3. The piezoresistive effect is most determined by the volume of the nanowires, and it usually responds in a linear way to the degree of strain. The piezotronic effect is an interface effect owing to the presence of the piezoelectric polarization charges at the interface. This is usually a nonlinear effect. Since ZnO is a piezoelectric semiconductor, a compressive strain generates piezo-charges at its interfacial region. The polarization charges are ionic and nonmobile located adjacent to the interface and thus cannot be completely screened. The positive piezoelectric charges may effectively lower the barrier height at the local Schottky contact (Φ_d); the negative piezoelectric charges increase the barrier height (Φ_s). Such a

tuning at the effective Schottky barrier height (SBH) would then greatly change the transport process of the device, which is defined as the piezotronic effect. This is the mechanism of the observed nanowire device in responding to strains. In this work, the piezoresistive effect is a "symmetric effect" regardless of the sign of the applied voltages, thus, it increased the output signals at both +1.1 V and −1.1 V in Figure 3 panels c−f. However, the piezotronic effect increased the output current at +1.1 V and decreased it at −1.1 V, because this effect has a polarity depending on the sign of the local piezoelectric charges. The obtained *I*−*V* curves of the ZnO NW device were a combination of piezoresistive effect and piezotronic effect, as reported in a previous work.[40] We now use the piezotronic effect to explain the data presented in Figure 4.

Energy band diagrams of the device are shown in Figure 7 to elucidate the piezotronic effect on drug metabolism and the improvement of sensing. Figure 7a presents the original state of the energy band diagram of a strain-free nanowire. There are two equivalent SBHs formed at both contacts in an M−S−M structure. Since the ZnO nanowire exhibits the piezoelectric effect, a strain applied on the nanowire along the *c*-axis would produce piezoelectric charges at the interfacial region. That is to say, a piezopotential exists inside the NW. Under this circumstance, free carriers can only partially screen the ionic piezoelectric charges but they cannot completely balance or neutralize out all of them. A positive piezopotential effectively lowers the local SBH at one end (Φ_D), while the negative piezopotential increases the local SBH at the other end (Φ_S) (Figure 7b). It has been proven that the transport process inside the ZnO NW is dominated by the reversely biased Schottky contact, that is Φ_D. Therefore, the local Φ_D becomes lower with an increase in the externally applied compressive strain, which results in a higher output current signal.

The working principle of the ZnO NW device decorated with CYP2C9/CPR microsomes is demonstrated by the corresponding energy band structure in Figure 7c−d for explaining the data presented in Figure 4b−e. When the CYP2C9/CPR microsomes were attached on the surface of the ZnO nanowire, the piezopotential produced by the compressively strained ZnO NW can promote electrons to transfer from CPR to CYP2C9, thus activating the active center of CYP2C9 consisting of heme proteins, as well as effectively change the local contact characteristics by an internal field, which makes the charge carrier easily go over the local barrier (Φ_D). So, the output signal increases. When the decorated ZnO NW was immersed into tolbutamide solution, the metabolism could proceed effectively. This should be ascribed to the activated CYP2C9, which prompted the target drug to perform a hydroxylation reaction. In the process of hydroxylation, essential electrons were provided by CYP2C9 (Figure 7d). In addition, more tolbutamide was metabolized, more electrons were transferred from CPR to CYP2C9 heme, then more electrons were transferred to the target drug from the CYP2C9 heme. That is to say, the more tolbutamide there was, the higher was the carrier density at the surface of ZnO NW device, and the higher was the current signal.[41] Furthermore, the hydrophobility of the ZnO NW promotes its combination with microsomes and promotes electrons to transfer from CPR to CYP2C9, then the active site of the isozyme is more easily activated.[42,43] With the presence of a strong local piezoelectric field provided by the piezoelectric polarization charges, electrons can be effectively transferred from CPR to CYP2C9. Therefore, the piezotronic effect can enhance drug metabolism on a single ZnO nanowire surface.

As for drug sensing, the modified SBH by piezotronic effect can maximize the sensor sensitivity; This occurs because the Schottky contacted device has been shown to exhibit much more sensitivity and response time than the Ohmic contacted devices for optical,[17] chemical,[44] gas,[45] and biochemical sensing.[46] This is the result presented in Figure 4d.

CONCLUSIONS

An M−S−M Schottky contacted ZnO NW device was fabricated as a drug metabolism driver. The piezotronic effect on the drug metabolism with a CYP2C9/CPR-microsomes decorated ZnO NW was systematically studied *via* varying both external compressive strain and target drug concentration. Our data indicate that the nonlinear effect introduced by the piezotronic effect in transport can significantly enhance the behavior of the device. That is to say, the device can not only improve the metabolism efficiency but also increase the sensitivity. What is more, HPLC−MS analyses were performed to demonstrate that the successful metabolism process generated 4-hydroxytolbutamide from tolbutamide. A theoretical model is presented for interpreting the observed behaviors of the device. The proposed self-powered approach in this work may have potential application in drug metabolism and trace drug analysis.

METHODS

Reagents. CYP 2C9 microsomes with CPR, CS, tolbutamide, and sulfaphenazole were obtained from Sigma-Aldrich Chemical Co. (St. Louis, MO). All other reagents used in this work were of A.R. grade from the Beijing Chemical Factory, China.

ZnO Micro/Nanowire Synthesis and Device Fabrication. ZnO nanowires were synthesized *via* the vapor−solid growth process.

ZnO powder was placed at the center of a tube furnace, while the alumina substrate was placed 25 cm downstream from the center. The synthesis temperature was 1400 °C at a pressure of 75 Torr for 3 h.

The ZnO NW devices were fabricated by transferring and binding individual ZnO NWs laterally onto polyethylene terephthalate (PET) substrates. Silver paste was used to fix the two ends of the NW, serving as the source and drain electrodes for the device, respectively. A thin layer of epoxy was used to cover both end-electrodes. This Ag−ZnO NW−Ag device is an M−S−M structure. To immobilize CYP2C9/CPR-microsomes on the surface of the ZnO NW, 2 μL of CS (0.5 wt %) and 5 μL of CYP2C9/CPR-microsomes solution containing 1 μM CYPs isozyme or 5 μL of 20 pM CYP2C9 isozyme solution were mixed together and drop-coated on the surface of the ZnO NW, then incubated for 1 h in the fume hood to dry naturally. The same process was repeated three times, followed by rinsing with PBS solution to remove the weakly adsorbed immobilized CYP2C9. The decorated ZnO NW was ready to perform drug metabolism.

Drug Metabolism Measurements. Piezotronic-effect enhanced drug metabolism measurements were performed on a synthesized function generator (Stanford Research Systems DS345) and a low noise current amplifier (Stanford Research Systems SR570). The stock solution of 50 μM drug required in the measurement was obtained by dissolving tolbutamide in methanol, which can minimize the effect of organic solvents on CYP activities. In the process of experiment, methanolic tolbutamide solution was added to 5 mM pH 7.4 phosphate-buffered solution (PBS) by a microsyringe.

Inhibition assay was conducted by the addition of different concentrations of inhibitor, sulfaphenazole into pH 7.4 PBS solution containing 4 μM tolbutamide. After each addition, the solution let sit for 30 min to render the inhibitor binding to CYP2C9.

HPLC, ESI−MS, Analyses. Separation of the metabolites was achieved by use of a HPLC system (Agilent 1200, USA) with a ZORBAX Eclipse XDB 150 mm × 2.1 mm of C18 column. A mobile phase consists of 40% methanol and 60% water with a flow rate of 0.3 mL/min at a wavelength of 230 nm. Five μL sample under test was obtained by collecting the solution after metabolism. In the process of ESI-MS, an Agilent 6400 mass spectrometer (Agilent, USA) worked in the positive ion mode under these conditions: gas temperature, 350 °C; gas flow, 8 L/min; nebulizer gas pressure, 45 psi; sheath gas temperature, 250 °C; sheath gas flow, 10 L/min; and capillary voltage, 4 kV.

Conflict of Interest: The authors declare no competing financial interest.

Acknowledgment. We thank the following for financial support: the National Natural Science Foundation of China (NSFC no. 21173017, 51272011 and 21275102), the Program for New Century Excellent Talents in University (NCET-12-0610), the science and technology research projects from the education ministry (213002A), National "Twelfth Five-Year" Plan for Science & Technology Support (No.2013BAK12B06), the "thousands talents" program for pioneer researcher and his innovation team, China, National Natural Science Foundation of China (Grant No. 51432005; No.Y4YR011001; No. 61204131), Beijing City Committee of Science and Technology (Z131100006013004, Z131100006013005).

REFERENCES AND NOTES

1. Klein, A. P.; Anarat-Cappillino, G.; Sattely, E. S. Minimum Set of Cytochromes P450 for Reconstituting the Biosynthesis of Camalexin, a Major Arabidopsis Antibiotic. *Angew. Chem., Int. Ed.* **2013**, *52*, 13625–13628.
2. Tripathi, S.; Li, H. Y.; Poulos, T. L. Structural Basis for Effector Control and Redox Partner Recognition in Cytochrome P450. *Science* **2013**, *340*, 1227–1230.
3. Danton, A. C.; Montastruc, F.; Sommet, A.; Durrieu, G.; Bagheri, H.; Bondon-Guitton, E.; Lapeyre-Mestre, M.; Montastruc, J. L. Importance of Cytochrome P450 (CYP450) in Adverse Drug Reactions Due to Drug−Drug Interactions: A PharmacoVigilance Study in France. *Eur. J. Clin. Pharmacol.* **2013**, *69*, 885–888.
4. Zamora, I.; Afzelius, L.; Cruciani, G. Predicting Drug Metabolism: A Site of Metabolism Prediction Tool Applied to the Cytochrome P450 2C9. *J. Med. Chem.* **2003**, *46*, 2313–2324.
5. Marchetti, S.; Mazzanti, R.; Beijnen, J. H.; Schellens, J. H. M. Concise Review: Clinical Relevance of Drug-Drug and Herb−Drug Interactions Mediated by the ABC Transporter ABCB1 (MDR1, P-glycoprotein). *Oncologist* **2007**, *12*, 927–941.
6. Grabowsky, J. A. Drug Interactions and the Pharmacist: Focus on Everolimus. *Ann. Pharmacother.* **2013**, *47*, 1055–1063.
7. Xu, X.; Wei, W.; Huang, M. H.; Yao, L.; Liu, S. Q. Electrochemically Driven Drug Metabolism *via* Cytochrome P450 2C9 Isozyme Microsomes with Cytochrome P450 Reductase and Indium Tin Oxide Nanoparticle Composites. *Chem. Commun.* **2012**, *48*, 7802–7804.
8. Nowak, P.; Wozniakiewicz, M.; Koscielniak, P. Simulation of Drug Metabolism. *Trac-Trend Anal. Chem.* **2014**, *59*, 42–49.
9. Sultana, N.; Schenkman, J. B.; Rusling, J. F. Protein Film Electrochemistry of Microsomes Genetically Enriched in Human Cytochrome P450 Monooxygenases. *J. Am. Chem. Soc.* **2005**, *127*, 13460–13461.
10. Krishnan, S.; Wasalathanthri, D.; Zhao, L. L.; Schenkman, J. B.; Rusling, J. F. Efficient Bioelectronic Actuation of the Natural Catalytic Pathway of Human Metabolic Cytochrome P450s. *J. Am. Chem. Soc.* **2011**, *133*, 1459–1465.
11. Rua, F.; Sadeghi, S. J.; Castrignano, S.; Di Nardo, G.; Gilardi, G. Engineering Macaca Fascicularis Cytochrome P450 2C20 to Reduce Animal Testing for New Drugs. *J. Inorg. Biochem.* **2012**, *117*, 277–284.
12. Schneider, E.; Clark, D. S. Cytochrome P450 (CYP) Enzymes and the Development of CYP Biosensors. *Biosens. Bioelectron.* **2013**, *39*, 1–13.
13. Krishnan, S.; Schenkman, J. B.; Rusling, J. F. Bioelectronic Delivery of Electrons to Cytochrome P450 Enzymes. *J. Phys. Chem. B* **2011**, *115*, 8371–8380.
14. Yoshioka, K.; Kato, D.; Kamata, T.; Niwa, O. Cytochrome P450 Modified Polycrystalline Indium Tin Oxide Film as a Drug Metabolizing Electrochemical Biosensor with a Simple Configuration. *Anal. Chem.* **2013**, *85*, 9996–9999.
15. Huang, M. H.; Xu, X.; Yang, H.; Liu, S. Q. Electrochemically-Driven and Dynamic Enhancement of Drug Metabolism *via* Cytochrome P450 Microsomes on Colloidal Gold/Graphene Nanocomposites. *RSC Adv.* **2012**, *2*, 12844–12850.
16. Ashfaq, M.; Khan, S.; Verma, N. Synthesis of PVA-CAP-Based Biomaterial *in Situ* Dispersed with Cu Nanoparticles and Carbon Micro-Nanofibers for Antibiotic Drug Delivery Applications. *Biochem. Eng. J.* **2014**, *90*, 79–89.
17. Wang, Z. L. Progress in Piezotronics and Piezo-phototronics. *Adv. Mater.* **2012**, *24*, 4632–4646.
18. Xiao, X.; Yuan, L. Y.; Zhong, J. W.; Ding, T. P.; Liu, Y.; Cai, Z. X.; Rong, Y. G.; Han, H. W.; Zhou, J.; Wang, Z. L. High-Strain Sensors Based on ZnO Nanowire/Polystyrene Hybridized Flexible Films. *Adv. Mater.* **2011**, *23*, 5440–5444.
19. Gedamu, D.; Paulowicz, I.; Kaps, S.; Lupan, O.; Wille, S.; Haidarschin, G.; Mishra, Y. K.; Adelung, R. Rapid Fabrication Technique for Interpenetrated ZnO Nanotetrapod Networks for Fast UV Sensors. *Adv. Mater.* **2014**, *26*, 1541–1550.
20. Liu, X.; Gu, L. L.; Zhang, Q. P.; Wu, J. Y.; Long, Y. Z.; Fan, Z. Y. All-Printable Band-Edge Modulated ZnO Nanowire Photodetectors with Ultra-High Detectivity. *Nat. Commun.* **2014**, *5*, 1–9.
21. Zhou, J.; Xu, N. S.; Wang, Z. L. Dissolving Behavior and Stability of ZnO Wires in Biofluids: A Study on Biodegradability and Biocompatibility of ZnO Nanostructures. *Adv. Mater.* **2006**, *18*, 2432–2435.
22. Li, Z.; Yang, R. S.; Yu, M.; Bai, F.; Li, C.; Wang, Z. L. Cellular Level Biocompatibility and Biosafety of ZnO Nanowires. *J. Phys. Chem. C* **2008**, *112*, 20114–20117.
23. Yang, C.; Xu, C. X.; Wang, X. M. ZnO/Cu Nanocomposite: A Platform for Direct Electrochemistry of Enzymes and Biosensing Applications. *Langmuir* **2012**, *28*, 4580–4585.

24. Park, H. Y.; Gedi, V.; Kim, J.; Park, H. C.; Han, S. H.; Yoon, M. Y. Ultrasensitive Diagnosis for an Anthrax-Protective Antigen Based on a Polyvalent Directed Peptide Polymer Coupled to Zinc Oxide Nanorods. *Adv. Mater.* **2011**, *23*, 5425–5429.
25. Wang, W. J.; Hao, Q.; Wang, W.; Bao, L.; Lei, J. P.; Wang, Q. B.; Ju, H. X. Quantum Dot-Functionalized Porous ZnO Nanosheets as a Visible Light Induced Photoelectrochemical Platform for DNA Detection. *Nanoscale* **2014**, *6*, 2710–2717.
26. Zhao, Z. W.; Lei, W.; Zhang, X. B.; Wang, B. P.; Jiang, H. L. ZnO-Based Amperometric Enzyme Biosensors. *Sensors* **2010**, *10*, 1216–1231.
27. Liu, T. Y.; Liao, H. C.; Lin, C. C.; Hu, S. H.; Chen, S. Y. Biofunctional ZnO Nanorod Arrays Grown on Flexible Substrates. *Langmuir* **2006**, *22*, 5804–5809.
28. Yue, H. Y.; Huang, S.; Chang, J.; Heo, C.; Yao, F.; Adhikari, S.; Gunes, F.; Liu, L. C.; Lee, T. H.; Oh, E. S.; Li, B.; Zhang, J. J.; Huy, T. Q.; Luan, N. V.; Lee, Y. H. ZnO Nanowire Arrays on 3D Hierachical Graphene Foam: Biomarker Detection of Parkinson's Disease. *ACS Nano* **2014**, *8*, 1639–1646.
29. Lee, J.; Choi, S.; Bae, S. J.; Yoon, S. M.; Choi, J. S.; Yoon, M. Visible Light-Sensitive APTES-Bound ZnO Nanowire toward a Potent Nanoinjector Sensing Biomolecules in a Living Cell. *Nanoscale* **2013**, *5*, 10275–10282.
30. Zhang, J.; Xiao, X. X.; He, Q. Q.; Huang, L. F.; Li, S.; Wang, F. A Nonenzymatic Glucose Sensor Based on a Copper Nanoparticle-Zinc Oxide Nanorod Array. *Anal. Lett.* **2014**, *47*, 1147–1161.
31. Zhou, J.; Gu, Y. D.; Fei, P.; Mai, W. J.; Gao, Y. F.; Yang, R. S.; Bao, G.; Wang, Z. L. Flexible Piezotronic Strain Sensor. *Nano Lett.* **2008**, *8*, 3035–3040.
32. Pan, Z. W.; Dai, Z. R.; Wang, Z. L. Nanobelts of Semiconducting Oxides. *Science* **2001**, *291*, 1947–1949.
33. Eichenfield, M.; Chan, J.; Camacho, R. M.; Vahala, K. J.; Painter, O. Optomechanical Crystals. *Nature* **2009**, *462*, 78–82.
34. Miners, J. O.; Birkett, D. J. Cytochrome P4502C9: An Enzyme of Major Importance in Human Drug Metabolism. *Br. J. Clin. Pharmacol.* **1998**, *45*, 525–538.
35. Yang, R. S.; Qin, Y.; Dai, L. M.; Wang, Z. L. Power Generation with Laterally Packaged Piezoelectric Fine Wires. *Nat. Nanotechnol* **2009**, *4*, 34–39.
36. Hansen, L. L.; Brosen, K. Quantitative Determination of Tolbutamide and Its Metabolites in Human Plasma and Urine by High-Performance Liquid Chromatography and UV Detection. *Ther. Drug Monit.* **1999**, *21*, 664–671.
37. Taylor, G. E.; Gosling, M.; Pearce, A. Low Level Determination of p-Toluenesulfonate and Benzenesulfonate Esters in Drug Substance by High Performance Liquid Chromatography/Mass Spectrometry. *J. Chromatogr. A* **2006**, *1119*, 231–237.
38. Kanamitsu, S.; Ito, K.; Sugiyama, Y. Quantitative Prediction of *in Vivo* Drug−Drug Interactions from *in Vitro* Data Based on Physiological Pharmacokinetics: Use of Maximum Unbound Concentration of Inhibitor at the Inlet to the Liver. *Pharm. Res.-Dordr.* **2000**, *17*, 336–343.
39. Mancy, A.; Dijols, S.; Poli, S.; Guengerich, F. P.; Mansuy, D. Interaction of Sulfaphenazole Derivatives with Human Liver Cytochromes P450 2C: Molecular Origin of the Specific Inhibitory Effects of Sulfaphenazole on CYP 2C9 and Consequences for the Substrate Binding Site Topology of CYP 2C9. *Biochemistry US* **1996**, *35*, 16205–16212.
40. Zhou, J.; Fei, P.; Gu, Y. D.; Mai, W. J.; Gao, Y. F.; Yang, R.; Bao, G.; Wang, Z. L. Piezoelectric-Potential-Control Led Polarity-Reversible Schottky Diodes and Switches of ZnO Wires. *Nano Lett.* **2008**, *8*, 3973–3977.
41. Yu, R. M.; Pan, C. F.; Chen, J.; Zhu, G.; Wang, Z. L. Enhanced Performance of a ZnO Nanowire-Based Self-Powered Glucose Sensor by Piezotronic Effect. *Adv. Funct. Mater.* **2013**, *23*, 5868–5874.
42. Mie, Y.; Suzuki, M.; Komatsu, Y. Electrochemically Driven Drug Metabolism by Membranes Containing Human Cytochrome P450. *J. Am. Chem. Soc.* **2009**, *131*, 6646–6647.
43. Willander, M.; Khun, K.; Ibupoto, Z. H. ZnO Based Potentiometric and Amperometric Nanosensors. *J. Nanosci. Nanotechnol.* **2014**, *14*, 6497–6508.
44. Pan, C. F.; Yu, R. M.; Niu, S. M.; Zhu, G.; Wang, Z. L. Piezotronic Effect on the Sensitivity and Signal Level of Schottky Contacted Proactive Micro/Nanowire Nanosensors. *ACS Nano* **2013**, *7*, 1803–1810.
45. Wei, T. Y.; Yeh, P. H.; Lu, S. Y.; Wang, Z. L. Gigantic Enhancement in Sensitivity Using Schottky Contacted Nanowire Nanosensor. *J. Am. Chem. Soc.* **2009**, *131*, 17690–17695.
46. Hansen, B. J.; Liu, Y.; Yang, R. S.; Wang, Z. L. Hybrid Nanogenerator for Concurrently Harvesting Biomechanical and Biochemical Energy. *ACS Nano* **2010**, *4*, 3647–3652.